Journal of Sustainability for Energy
https://www.acadlore.com/journals/JSE

Enhancing Heat Transfer in Heating Pipes with Fe_3O_4 Nanofluid under Magnetic Fields: A Numerical Study

Asaad Abdulnabi Lazim[1], Alireza Daneh-Dezfuli[1],Laith Jaafer Habeeb[2*]

[1] Mechanical Engineering Department, Faculty of Engineering, Shahid Chamran University of Ahvaz, 63 Ahvaz, Iran
[2] Training and Workshop Center, University of Technology-Iraq, 10001 Baghdad, Iraq

* Correspondence: Laith Jaafer Habeeb (Laith.J.Habeeb@uotechnology.edu.iq)

Received: 10-20-2023 **Revised:** 12-02-2023 **Accepted:** 12-10-2023

Citation: A. A. Lazim, A. Daneh-Dezfuli, and L. J. Habeeb, "Enhancing heat transfer in heating pipes with Fe_3O_4 nanofluid under magnetic fields: A numerical study," *J. Sustain. Energy*, vol. 2, no. 4, pp. 207–216, 2023. https://doi.org/10.56578/jse020404.

Abstract: In this investigation, the enhancement of heat transfer in pipes facilitated by Fe_3O_4-distilled water nanofluid under the influence of magnetic fields is comprehensively studied. The research primarily focuses on examining the alterations in the thermal boundary layer and fluid flow patterns caused by the application of magnetic fields. It is observed that magnetic fields induce the formation of vortexes, thereby actively influencing the flow patterns within the fluid. These vortexes play a pivotal role in promoting thermal diffusion, resulting in an improved heat transfer rate. The core aim of this study is to quantitatively assess the impact of magnetic nanofluids on the coefficient of heat transfer. A model tube, possessing an inner diameter of 25.4 mm and a length of 210 mm, serves as the basis for the simulations. The investigation encompasses a range of inlet velocities (0.05, 0.1, and 0.5 m/s) and exit pressures to analyze the magnetic field's effect on heat transfer and fluid dynamics. Magnetic flux intensities of one, two, and three Tesla are employed. Notably, the highest temperature of 349 K is recorded in the presence of three magnets, indicating an escalation in temperature with an increase in magnetic strength. However, a diminishing temperature rise is noted over a specified distance with additional magnets. For instance, at a distance of 100 mm, the temperature peaks at 340 K with one magnet, whereas with two magnets, this temperature is attained at a mere 50 mm, suggesting enhanced magnetizer efficiency. Furthermore, the introduction of a magnetic field at the tube's center reveals that high flow velocities tend to counteract the magnetic influence due to their superior force, which impedes the incorporation of metal particles into the fluid. As the magnetic flux value escalates, the nanofluid's magnetic particles either congregate or disperse, thereby obstructing flow and intensifying channel vortices. This phenomenon results in heightened turbulence, instigated by the magnets, which in turn precipitates a rapid increase in fluid flow velocity, thereby impeding the fluid's capacity to adequately absorb heat for efficient heating.

Keywords: Magnetic materials; Nanofluid dynamics; Thermal analysis; Vortex formation; Magnetic field interaction; Heat transfer enhancement

1 Introduction

Heat transfer is a crucial topic in various industries, including manufacturing, construction, and transportation. Small coolers and heat exchangers with high heat transfer rates are essential. Improving heat transfer techniques with high coefficient rates and compact design is essential for increased efficiency. Magnetic hyperthermia is used for cancer treatment, and a ferrofluid is used to improve heat transfer. Magnetic fluids are magnetic nanoparticles in a Newtonian liquid carrier, often made of magnetite, heptane, or long-chain hydrocarbons. They exhibit Brownian motion (Brownian motion is the random movement of particles suspended in a medium, consisting of fluctuations in a particle's position within a fluid sub-domain, followed by relocation to another sub-domain, and more fluctuations within the new closed volume.) due to their small size and magnetism. Their intensity depends on factors like volume percentage, viscosity, temperature, saturation magnetization, and applied field strength [1–3]. Nanoparticle creation is a biological technique using microbes and enzymes to create nanoparticles. The addition of nanoparticles to a fluid can alter its thermal and rheological properties. Nanofluids have a two-phase nature, making them difficult to combine. The main goal is to maintain long-term dispersion stability without affecting properties [4, 5]. Magnetic materials

are classified into diamagnetic, paramagnetic, ferromagnetic, anti-ferromagnetic, and ferrimagnetic. Magnetic susceptibility (In electromagnetism, it refers to the degree to which a material becomes magnetized in an applied magnetic field.) measures a material's magnetization response to an applied magnetic field. Both diamagnetic and paramagnetic materials display no hysteresis at ambient temperature. Diamagnetism occurs when a substance has a minimal net magnetic moment. Magnetic permeability (the capacity of a material to let liquids or gases pass through it) measures a substance's ability to develop high magnetization in mild magnetic fields. Paramagnetic materials with atomic moment disorder produce no net magnetization. Fe_3O_4 nanoparticles, with their high saturation magnetization value at normal temperature, are a crucial additive due to their high importance [6–12]. The study investigates the impact of a magnetic field on the flow of nanofluid within a two-tube sinusoidal heat exchanger (sinusoidal corrugated plate heat exchanger). The base fluid is water containing 4% nanoparticles (Fe_3O_4) magnetic field. The research found that the sinusoidal construction of the interior tube enhances the Nusselt number and promotes the diffusion of the cold border layer into the inner tube. Mousavi et al. [13] also found that the Nusselt number and heat transmission increase with higher field magnetism strengths. Goshayeshia et al. [14] examined the impact of Fe_2O_3/Kerosene nanofluid on a copper heat pipe under a field magnet. The study found that Fe_2O_3 nanoparticles improved the pipe's thermal resistance and heat transfer coefficient, especially in the presence of a magnetic field. The heat pipe's performance was significantly influenced by the inclination angle, with a critical angle of 75°. Rashidiab et al. [15] looked at how heat moved through nanofluids using mixed convection in a vertical tube with sinusoidal walls while a magnetic field was present. It examined heat transport and hydrodynamic properties using various amplitudes and Hartman numbers (which equal the product of the magnetic flux density). The study found that increasing the Grashof number (a dimensionless number that roughly represents the fluid's buoyancy to viscous force ratio) and Reynolds number increased the average Nusselt number and Poiseuille number. Sheikholeslamia et al. [16] simulated CuO-H_2O nanofluid flow in a permeable channel using the Lattice Boltzmann technique, and their paper examines a homogeneous model, considering Brownian motion. Results show that increasing porous medium permeability increases heat transmission rate, and temperature boundary layer thickness increases with magnetic field. Gandomkara et al. [17] aimed to improve the heat transfer performance of ferrofluid PHP by examining its behavior in copper and glass heat pipes. Results showed that ferrofluid PHP is more stable in glass environments and that magnetic field improves performance in copper PHP, while increasing ferrofluid concentration enhances performance in glass PHP under all field magnetism application situations. Jiao et al. [18] investigated the flow and convective heat transfer properties of ferrofluids in tubes subjected to magnetic fields. The results showed that the magneto-viscous effects of external fields outweighed any potential increase in convective heat transmission, indicating that ferrofluids may not be suitable for heat transfer in high-magnetic fields. Jiao et al. [19] examined the impact of graphene oxide and supergraphene nanoparticles on the performance of a mini radiator. Results showed that at 0.4 vol.% of hybrid nanofluids, the Nusselt number increased by 5.62 times, and efficacy and pressure drop improved. Functionalized graphene has potential for improving mini radiator performance. Multi-wall carbon nanotubes (MWCNTs) are nanoparticles that improve thermal behavior in base fluids. They are used in micro-polar nanofluids, where micro-rotation is considered.

The study focuses on a new model with an inner flow diameter of 25.4 mm and a tube length of 210 mm. The shed locations for magnets are evenly distributed on the tube's surface, with a 45 mm gap between each and a 10 mm width. Heat is shed on the wall's outer layer. The limitations indicate nanomaterial entry at 300 K with entry velocities of (0.05, 0.1, 0.5) m/s. When the middle magnet is turned on, an exit pressure of 0 Pa is delivered to the heat surfaces, and a constant temperature of 350 K is shed. Three Tesla magnetic flux forces are selected.

2 Aim of Study

The research aims to analyze the flow and enhancement of heat transfer in Fe_3O_4-distilled water in a tube with a magnetic field by simulating part of the problem with the Fluent package under ANSYS and studying the magnetic field's influence on magnetic nanofluid to increase heat transfer rate.

(1) The study focuses on determining wall temperature, inlet and outlet nanofluid temperatures, heat flux, flow rate, and pressure drop in turbulent flow regimes.

(2) Examine the impact of increasing the nanofluid concentration on the transmission of heat rate and flow with a uniform heat flux section.

(3) The study aims to investigate the behavior of magnetic nanofluid to estimate the increase in the coefficient of heat transfer.

3 Theoretical Part

This paragraph will go over all of the fundamental equations that were used to get the findings from the numerical component, as well as the programs and configurations needed to provide accurate and trustworthy results. Studies in computational fluid dynamics (CFD) are conducted to get deeper insights into the area of the stream. The (k-ε) model is used to describe the effects of the disturbance model, which incorporates the configuration of a two-component

condition. Consequently, these Cartesian direction coordinates will be addressed by the mathematical arrangement techniques (*x*, *y*, and *z*). A computation for three-dimensional geometry is developed. The simulation tool ANSYS (20.1) was used to resolve the scenarios. The running nanofluid in the current work is supposed to consist of Fe_3O_4 and water with certain flow parameters (steady flow, three-dimensional, Newtonian, incompressible, and turbulent). The magnetic field produced by the permanent magnets in the situation under study is nearly uniform. Consequently, there will be a homogeneous flux in the magnetic body force. The magnetic vortex generator's primary parts are magnetite ferrofluid and permanent magnets. Three permanent magnets that are positioned all around the pipe make up the vortex generator. In order to replicate the magnetic field, ANSYS uses a User-Defied Function (UDF).

3.1 Standard k-ε Model

The k-ε standard model is a widely used model for analyzing disturbance dynamics and dispersal rates in turbulent streams. It is based on specific vehicle conditions and assumes the stream is fierce, with subatomic thickness effects being insignificant. The model's benefits and drawbacks have been revealed, with the turbulent nature of the dynamic energy and scattering rate derived from specific vehicle conditions.

$$\frac{\partial}{\partial t}(\rho k) + \frac{\partial}{\partial x_i}(\rho k u_i) = \frac{\partial}{\partial x_j}\left[\left(\mu + \frac{\mu_t}{\sigma_k}\right)\frac{\partial k}{\partial x_j}\right] + G_k + G_b - \rho\varepsilon - Y_M + S_k \tag{1}$$

and

$$\frac{\partial}{\partial t}(\rho\varepsilon) + \frac{\partial}{\partial x_i}(\rho\varepsilon u_i) = \frac{\partial}{\partial x_j}\left[\left(\mu + \frac{\mu_t}{\sigma_\varepsilon}\right)\frac{\partial \varepsilon}{\partial x_j}\right] + C_{1\varepsilon}\frac{\varepsilon}{k}(G_k + C_{3\varepsilon}G_b) - C_{2\varepsilon}\rho\frac{\varepsilon^2}{k} + S_\varepsilon \tag{2}$$

In the text, the age of turbulent active energy, disturbance dynamic energy due to lightness, and the contribution of changing dilatation in compressible disturbance to the overall scattering rate are all talked about. It also discusses the violent Prandtl numbers for *k* and ε and the turbulent viscosity.

$$\mu_t = \rho C_\mu \frac{k^2}{\varepsilon} \tag{3}$$

where, C_μ is a constant

The model constants are $C_{1\varepsilon}$, $C_{2\varepsilon}$, C_μ, σ_k, and σ_ε, and they have the following default values:

$$C_{1\varepsilon} = 1.44, C_{2\varepsilon} = 1.92, C_\mu = 0.09, \sigma_k = 1.0, \sigma_\varepsilon = 1.3 \tag{4}$$

The default values for turbulent streams, including limit layers, blending layers, planes, and Standard, RNG, and Realizable k-ε Models for rotting isotropic matrix disturbance, function well for various limited and free shear streams.

3.2 Momentum Equations

In an inertial reference frame, momentum is conserved.

$$\frac{\partial}{\partial t}(\rho\vec{v}) + \nabla\cdot(\rho\vec{v}\vec{v}) = -\nabla p + \nabla\cdot(\bar{\bar{\tau}}) + \rho\vec{g} + \vec{F} \tag{5}$$

The static strain, pressure tensor, gravitational and outer body powers, and other model-subordinate source terminology are all included in the pressure tensor $\bar{\bar{\tau}}$.

$$\bar{\bar{\tau}} = \mu\left[\left(\nabla\vec{v} + \nabla\vec{v}^T\right) - \frac{2}{3}\nabla\cdot\vec{v}I\right] \tag{6}$$

The subatomic thickness, represented by *I*, is influenced by volume widening, as shown in the second component on the right-hand side.

3.3 Turbulence Model

The (k-ε) model efficiently reproduces hotness movement by considering tempestuous motor energy and violent dispersal rate, and calculating whirlpool consistency based on these factors.

3.4 Mesh Generation

The study utilized unstructured tetrahedron grids for complex geometries, utilizing ANSYS for solid geometry mesh generation and three-dimensional models with minimal user input as shown in Figure 1. The heat pipe is exposed to three magnetic fields (1, 2, and 3) to show the heat performance along the pipe.

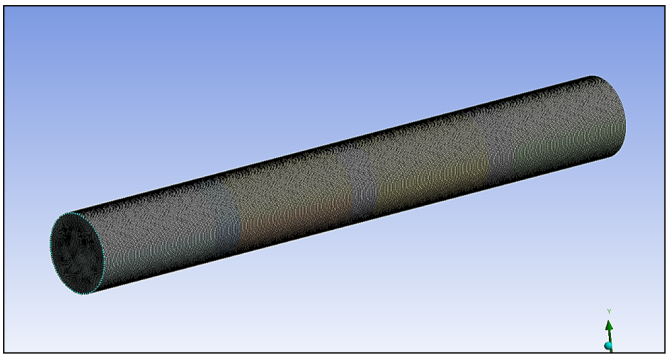

Figure 1. Mesh generated

Mesh independence is crucial for accurate and reliable results, stopping when output stability is reached with a 0.0005 m element size as shown in Table 1.

Table 1. Mesh independence

Case	Node	Element	Max. Temperature (K)	Outlet Temperature (K)	Pressure Difference (pa)
1	634212	523421	335.812	346.31	0.0455
2	1063643	974323	331.493	343.99	0.0394
3	1304363	1243667	329.081	343.81	0.0379
4	1505772	1451380	329.074	343.79	0.0378

3.5 Boundary Conditions

Figure 2 displays entry and exit velocities for nanomaterial entry at 300 K, exit pressure of 0 Pa at 350 K, and three cases of magnets with different forces of magnetic flux (1, 2, and 3) tesla.

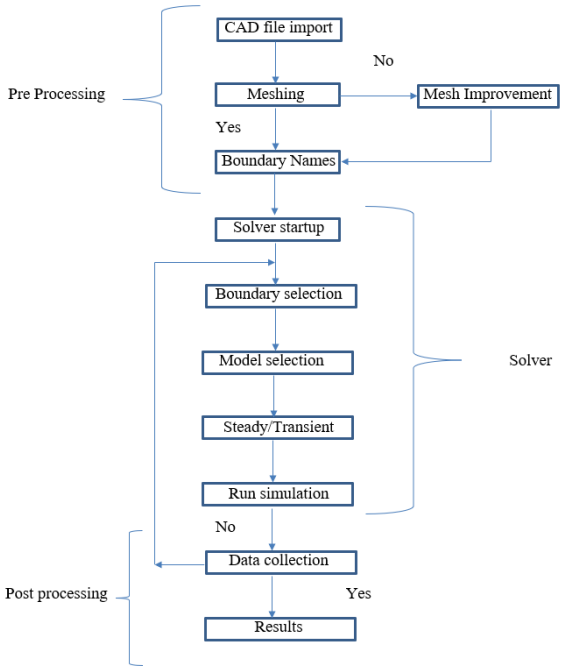

Figure 2. Flow chart of CFD

3.6 Problem Solution

The control-dependent technique involves creating a field network, building conditions like speed, pressure, and preserved scalars, and linearizing and iteratively tackling discretized equations. FLUENT uses ANSYS for arrangement calculation, which is used in this work. Consecutive, non-straight, and coupled conditions may take multiple cycles.

3.7 Solution Parameters

The solution parameters consist of the following:

A. Precision solver type

Accuracy solvers typically use single and twofold methods, with limitless accuracy causing residuals to zero, while genuine PCs adjust residuals and level them out.

B. Iterations number

The highest number of iterations completed before the solver terminates.

3.8 Convergence Criteria

The liquid stream conditions must be arranged with emphasis according to the CFD method until they are satisfied. When the arrangement stays within the precision of the selected blending models, the emphasis ceases. The mistake residuals, which are the difference between a variable's upsides in two continuous emphases standardized by the largest outright leftover for the first five cycles, are the most widely used method to check arrangement combinations. When the residuals for all previously introduced liquid stream conditions fall below a resilience breaking point of 10–6, the arrangement is expected to come together.

4 Results and Discussion

This paragraph reviews and discusses simulation program results, focusing on the effects of magnet number, magnetic field, and fluid entry velocity.

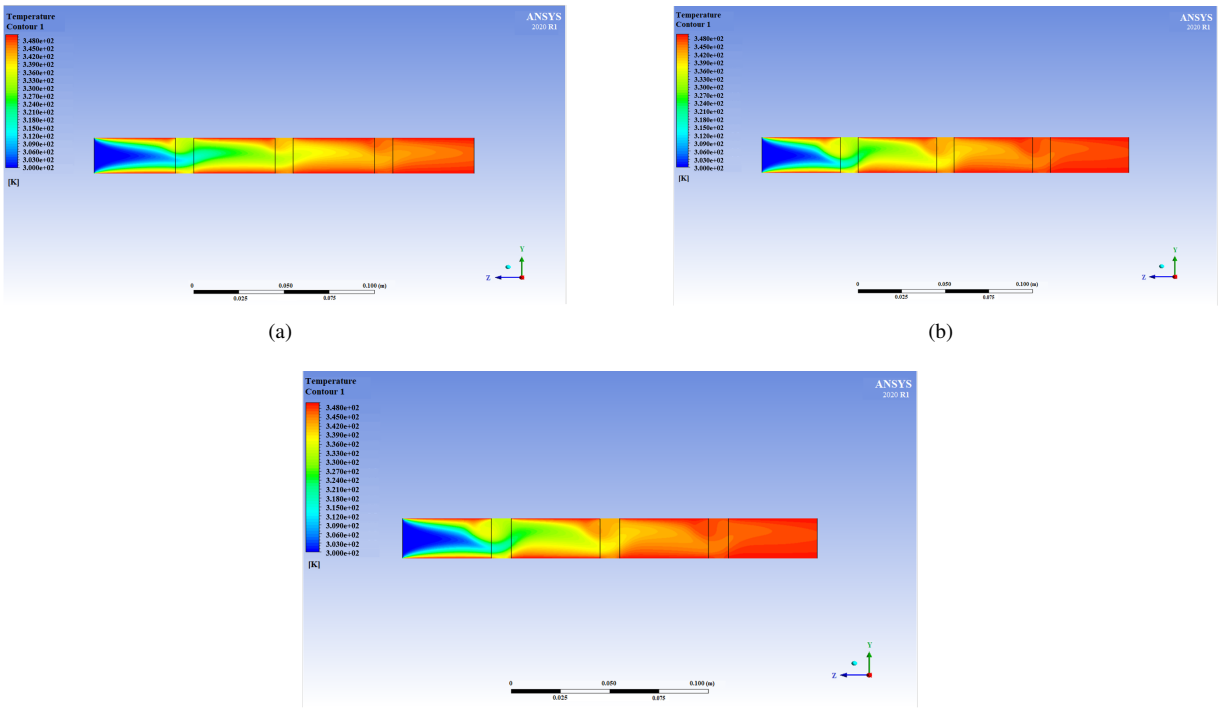

(a) (b)

(c)

Figure 3. Temperature contour at inlet velocity 0.05 m/s and 3 magnets (a) 1 Tesla; (b) 2 Tesla; (c) 3 Tesla

4.1 The Impact of Magnets' Magnetic Properties on Vortex Flow and Exit Temperature

The magnetic field's direction affects the movement of magnetized fluid, increasing turbulence. The increase in the value of the magnetic flux increases the instantaneous movement of the magnetized fluid and increases its turbulence. The exit temperature, 349.324 K, shows the largest amount of heat due to increased turbulence as shown in Figure 3.

Figure 4, Figure 5 and Figure 6 show that the exit temperature increases with the number of magnetic coils and magnetic flux and is inversely proportional to the velocity of fluid ingress.

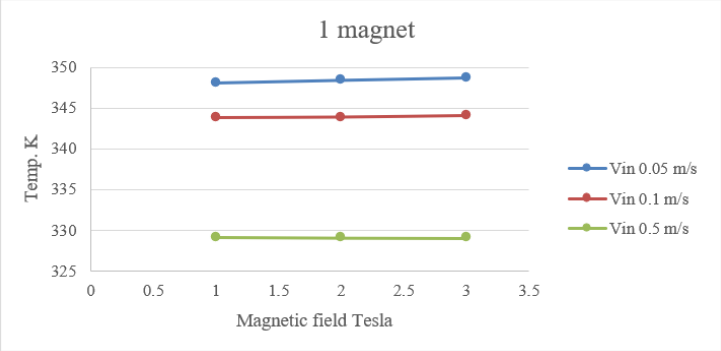

Figure 4. Temperature with magnetic field at 1 magnet

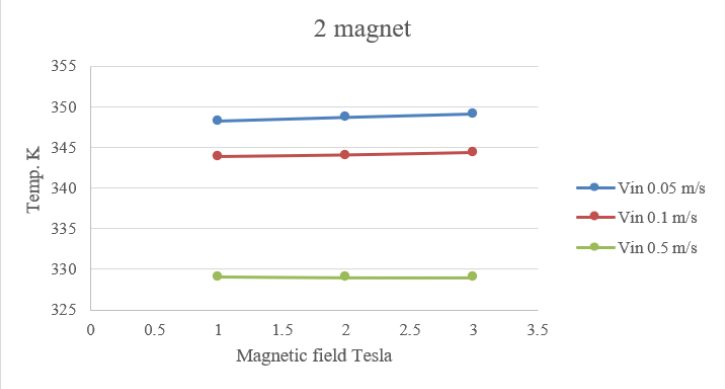

Figure 5. Temperature with magnetic field at 2 magnets

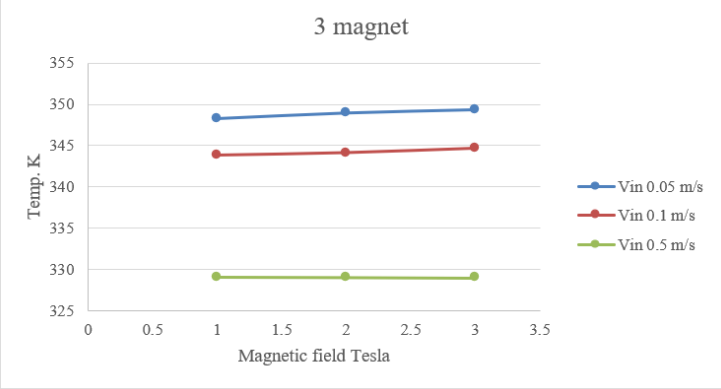

Figure 6. Temperature with magnetic field at 3 magnets

The magnetic flux increases velocity vortices by attracting or repelling magnetic material particles in the fluid, obstructing flow and increasing channel vortices, as shown in Figure 7.

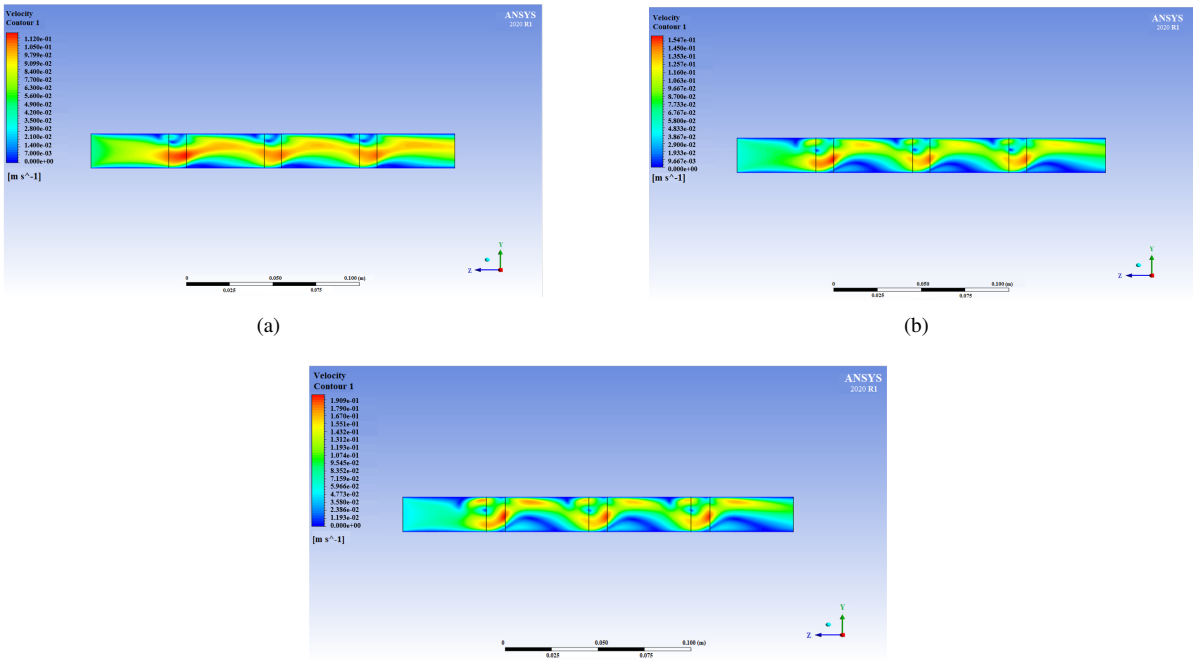

(a) (b)

(c)

Figure 7. Velocity contour at inlet velocity 0.05 m/s and 3 magnets. (a) 1 Tesla; (b) 2 Tesla; (c) 3 Tesla

4.2 Examination of the Pipe's Temperature Gradient

The temperature grading along the tube is crucial for understanding its physical state. Figure 8 and Figure 9 show that the temperature at the exit increases with an increase in magnetic field, reaching 348 K with an entry velocity of 0.05 m/s.

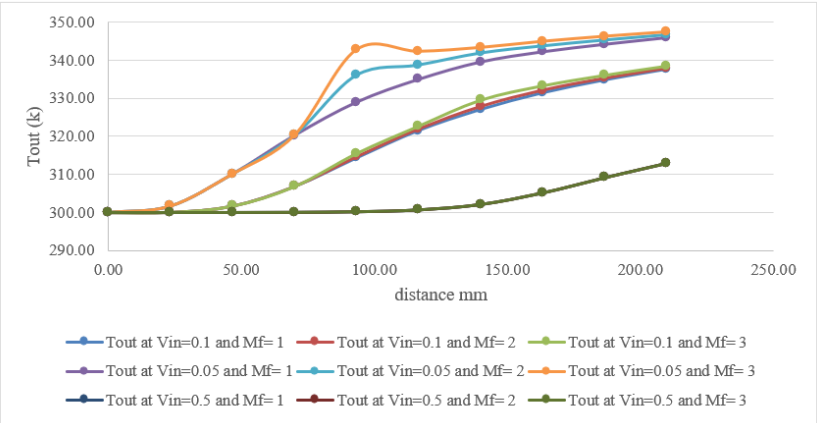

Figure 8. Temperature gradient along the pipe with 1 magnet

The number of magnets increases the temperature rise over a distance, with shorter temperature rises at 100 mm distances. Increased magnetizer efficiency increases temperature at 50 mm distances. Using three magnets and a magnetic field in the middle, the temperature rises in the tube as shown in Figure 10.

The Lorentz force is activated when a magnetic field is applied. The direction of the fluid flow and the magnetic field are both perpendicular to this force's action. The convective heat transfer inside the pipe can be improved, and additional fluid motion can be induced by the Lorentz force. Because of the Lorentz force, adding a magnetic field can cause more fluid motion. This increased flow of fluid results in an increased rate of convective heat transfer. An increase in magnetic field strength may cause the nanofluid turbulence to increase. Compared to laminar flow, turbulent flow is known to improve heat transfer because it encourages better fluid mixing and lowers the thermal boundary layer. A higher convective heat transfer coefficient is the result of the magnetic field's increased turbulence and fluid motion. This indicates that more heat from the heating pipe can be absorbed and removed by the nanofluid.

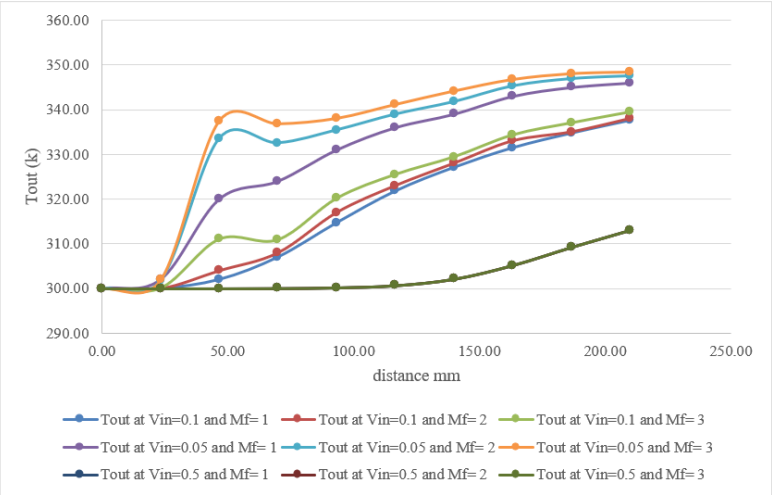

Figure 9. Temperature gradient along the pipe with 2 magnets

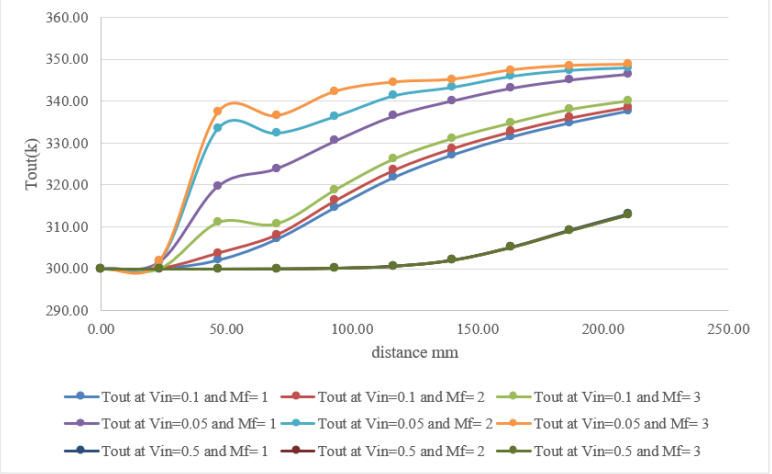

Figure 10. Temperature gradient along the pipe with 3 magnets

4.3 Compare with Previous Research

This study compares previous research on ferromagnetic materials using a geometry with inlet and outlet channels and a circular chamber as shown in Figure 11. A neodymium-iron-boron permanent magnet cube is placed next to the chamber to study the magnetic field effect. Diluted water-based ferrofluid is fed into the device, and the magnetic field magnitude is measured. The flow rate ranges from 50 to 400 μL/min [20].

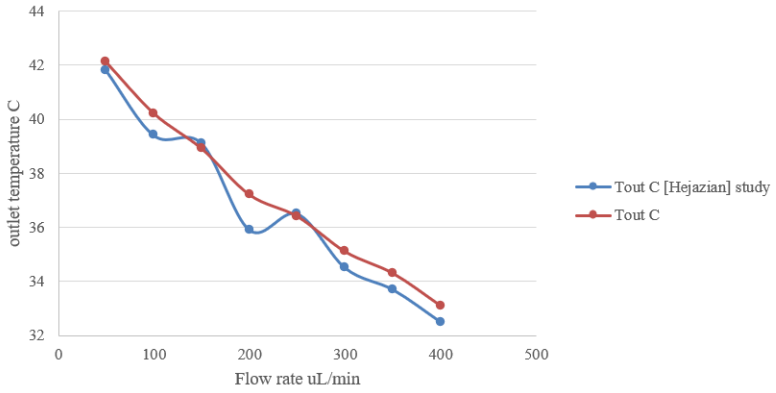

Figure 11. Outlet temperature at C with range of flow rate

5 Conclusions and Recommendations

The following conclusions can be drawn from the present work:

(1) The exit temperature rises with an increase in magnetic flux and is inversely proportional to the velocity of fluid ingress. Overall, thermal resistance falls as the heat transfer coefficient rises. As a result, heat is transferred from the pipe to the nanofluid more effectively, raising the temperature at the exit. A higher exit temperature is a result of this because the heat is removed from the heating pipe more effectively.

(2) Tesla's theory suggests that an increase in magnetic flux leads to an increase in the instantaneous movement of the magnetized fluid and its turbulence. In conclusion, increased fluid motion, turbulence, and convective heat transfer result from the strengthening of the magnetic field's interaction with the Fe_3O_4 nanofluid. The optimization of heat transfer in such systems is largely dependent on the combined effects of magnetic fields and nanofluid properties.

Recommendations for future work are:

(1) This procedure can utilize various nanofluid materials like Al_2O_3, TiO_2, and carbon nanotubes.

(2) Optimize the magnetic field intensity that can be applied to the nanofluid with a wide range.

(3) A fin-tube heat exchanger, a flat tube, and a vertical rectangular duct are three designs that can be used instead of pipes.

Data Availability

The data used to support the research findings are available from the corresponding author upon request.

Conflicts of Interest

The authors declare no conflict of interest.

References

[1] A. Asadi, A. H. Nezhad, F. Sarhaddi, and A. H. Keykha, "Laminar ferrofluid heat transfer in presence of non-uniform magnetic field in a channel with sinusoidal wall: A numerical study," *J. Magn. Magn. Mater.*, vol. 471, pp. 56–63, 2019. https://doi.org/10.1016/j.jmmm.2018.09.045

[2] S. F. Hosseinizadeh, S. Majidi, M. Goharkhah, and A. Jahangiri, "Energy and exergy analysis of ferrofluid flow in a triple tube heat exchanger under the influence of an external magnetic field," *Therm. Sci. Eng. Prog.*, vol. 25, p. 101019, 2021. https://doi.org/10.1016/j.tsep.2021.101019

[3] R. G. Gontijo, "Heat transfer increase for a laminar pipe flow of a magnetic fluid subjected to constant heat flux: An initial theoretical approach," *Mech. Res. Commun.*, vol. 91, pp. 27–32, 2018. https://doi.org/10.1016/j.mechrescom.2018.05.005

[4] A. Shahsavar, M. Saghafian, M. R. Salimpour, and M. B. Shafii, "Experimental investigation on laminar forced convective heat transfer of ferrofluid loaded with carbon nanotubes under constant and alternating magnetic fields," *Exp. Therm. Fluid. Sci.*, vol. 76, pp. 1–11, 2016. https://doi.org/10.1016/j.expthermflusci.2016.03.010

[5] Z. Narankhishig, J. Ham, H. Lee, and H. Cho, "Convective heat transfer characteristics of nanofluids including the magnetic effect on heat transfer enhancement - A review," *Appl. Therm. Eng.*, vol. 193, p. 116987, 2021. https://doi.org/10.1016/j.applthermaleng.2021.116987

[6] X. L. Zhang and Y. L. Zhang, "Heat transfer and flow characteristics of Fe_3O_4-water nanofluids under magnetic excitation," *Int. J. Therm. Sci.*, vol. 163, p. 106826, 2021. https://doi.org/10.1016/j.ijthermalsci.2020.106826

[7] X. L. Zhang and Y. L. Zhang, "Experimental study on enhanced heat transfer and flow performance of magnetic nanofluids under alternating magnetic field," *Int. J. Therm. Sci.*, vol. 164, p. 106897, 2021. https://doi.org/10.1016/j.ijthermalsci.2021.106897

[8] Y. Sheikhnejad, R. Hosseini, and M. Saffar-Avval, "Effect of different magnetic field distributions on laminar ferroconvection heat transfer in horizontal tube," *J. Magn. Magn. Mater.*, vol. 389, pp. 136–143, 2015. https://doi.org/10.1016/j.jmmm.2015.04.029

[9] H. H. Lua, Z. J. Wanga, D. Yun, J. Li, and Z. W. Shan, "A new approach of using Lorentz force to study single-asperity friction inside TEM," *J. Mater. Sci. Technol.*, vol. 84, pp. 43–48, 2021. https://doi.org/10.1016/j.jmst.2020.12.044

[10] B. Xiang, H. Liu, and Y. J. Yu, "Gimbal effect of magnetically suspended flywheel with active deflection of Lorentz-force magnetic bearing," *Mech. Syst. Signal. Process.*, vol. 173, p. 109081, 2022. https://doi.org/10.1016/j.ymssp.2022.109081

[11] J. H. Cheng, L. W. Cheng, and C. Y. Chen, "Flow transition of magneto hydrodynamic bubbly jet driven by Lorentz force," *J. Taiwan Inst. Chem. Eng.*, vol. 135, p. 104369, 2022. https://doi.org/10.1016/j.jtice.2022.104369

[12] A. A. Karamallah, L. J. Habeeb, and A. H. Asker, "The effect of magnetic field with nanofluid on heat transfer in a horizontal pipe," *Al-Khwarizmi Eng. J.*, vol. 12, no. 3, pp. 99–109, 2016.

[13] S. V. Mousavi, M. Sheikholeslami, and M. B. Gerdroodbary, "The Influence of magnetic field on heat transfer of magnetic nanofluid in a sinusoidal double pipe heat exchanger," *Chem. Eng. Res. Des.*, vol. 113, pp. 112–124, 2016. https://doi.org/10.1016/j.cherd.2016.07.009

[14] H. R. Goshayeshia, M. Goodarzic, M. R. Safaeic, and M. Daharib, "Experimental study on the effect of inclination angle on heat transfer enhancement of a ferrofluid in a closed loop oscillating heat pipe under magnetic field," *Exp. Therm. Fluid Sci.*, vol. 74, pp. 265–270, 2016. https://doi.org/10.1016/j.expthermflusci.2016.01.003

[15] M. M. Rashidiab, M. Nasiric, M. Khezerlooc, and N. Laraqid, "Numerical investigation of magnetic field effect on mixed convection heat transfer of nanofluid in a channel with sinusoidal walls," *J. Magn. Magn. Mater.*, vol. 401, pp. 159–168, 2016. https://doi.org/10.1016/j.jmmm.2015.10.034

[16] M. Sheikholeslamia, S. A. Shehzadb, and Z. X. Li, "Nanofluid heat transfer intensification in a permeable channel due to field magnetism using lattice Boltzmann method," *Physica B Condens. Matter*, vol. 542, pp. 51–58, 2018. https://doi.org/10.1016/j.physb.2018.03.036

[17] A. Gandomkar, M. Saidi, M. Shafii, M. Vandadi, and K. Kalan, "Visualization and comparative investigations of pulsating ferro-fluid heat pipe," *Appl. Therm. Eng.*, vol. 116, pp. 56–65, 2017. https://doi.org/10.1016/j.applthermaleng.2017.01.068

[18] F. Jiao, Q. Li, Y. Y. Jiao, and Y. Q. He, "Heat transfer of ferrofluids with magnetoviscous effects," *J. Mol. Liq.*, vol. 328, p. 115404, 2021. https://doi.org/10.1016/j.molliq.2021.115404

[19] F. Jiao, Q. Li, and Y. Q. He, "Electromotive force induced by the moving non-magnetic phase in ferrofluids," *Sens. Actuators A Phys.*, vol. 317, p. 112472, 2021. https://doi.org/10.1016/j.sna.2020.112472

[20] M. Hejazian and N. T. Nguyen, "Magnetofluidics for manipulation of convective heat transfer," *Int. Commun. Heat Mass Transf.*, vol. 81, pp. 149–154, 2017. https://doi.org/10.1016/j.icheatmasstransfer.2016.12.017